RESEARCH

Comparative performance investigation of a dual evaporator cycle using an ejector with the conventional cycle using a pressure reducing valve

Gulshan Sachdeva[1], Ajay Jaiswar[1], Parinam Anuradha[2] and Vaibhav Jain[3]*

Abstract

The performance of a dual evaporator cycle using ejector is compared with a conventional cycle employing pressure reducing valve. In both the systems, high temperature evaporator is considered as a flooded evaporator, thus a separator is employed after the high temperature evaporator. However, low temperature evaporator is a kind of conventional dry evaporator. The comparison of both systems, i.e., conventional and ejector assisted, is done for the same cooling capacities and same dryness fraction at the exit of high temperature evaporator with R134a, R152a, and R1234yf refrigerants. The effects of varying the states of refrigerant at the exit of flooded evaporator, and temperatures of both the evaporators and the condenser are analyzed using Engineering Equation Solver. It is found that the compressor work is reduced in both the cycles with the rise in low temperature evaporator temperature; however, a little variation is observed in the total cooling effect. The cooling effect in high temperature evaporator is increased with the increase in dryness fraction at the exit of the high temperature flooded evaporator, but it is decreased in low temperature evaporator.

Keywords Dual evaporator, VCRC, Ejector, Pressure reducing valve, COP

1 Introduction

A refrigerating or air conditioning system working on the most commercialized vapor compression system requires a considerable amount of high grade energy for its operation. The demand of these energy guzzlers has also been multiplying day by day. Therefore, researchers have been putting efforts in reducing the energy consumption of these vapor compression cooling systems. Robinson and Groll [1] explained that the throttling device was responsible for a considerable fraction of total irreversibility

while working with carbon dioxide as refrigerant. They found that the throttling contribution to total irreversibility could be reduced by 35% with the use of a turbine of even 60% isentropic efficiency. The options to reduce the throttling losses have been explored intensively for many years. The ejector has been examined as a viable substitute of conventional pressure reducing valve in the compression cooling systems. An ejector is a simple, static component wherein a high-pressure fluid is expanded reversibly at constant entropy unlike the irreversible isenthalpic expansion in the conventional expansion devices. Moreover, the ejector retrieves a fraction of the lost expansion work in its diffuser, thus has a potential to improve the performance.

In 1990, Kornhauser [2] for the very first time analyzed numerically the application of an ejector as a throttling device in a vapor compression system. He recorded 21%

*Correspondence:
Vaibhav Jain
vaibhavursaathi@gmail.com
[1] National Institute of Technology Kurukshetra, Thanesar, India
[2] U.I.E.T., Kurukshetra University, Thanesar, India
[3] Maharaja Agrasen Institute of Technology, Delhi, India

Sachdeva *et al. Int. J. Air-Cond. Ref.*   (2023) 31:20

Page 2 of 16

enhancement in COP with the proposed system over a standard vapor compression system using R12 refrigerant at 30 ℃ and − 15 ℃ condenser and evaporator temperatures respectively. However, Kornhauser and Harrel [3] could obtain only 3.9 to 7.6% rise in the COP while conducting experiments with R134a. Sarkar [4] numerically studied the ejector vapor compression system (EVCS) using constant pressure ejector model for propane, ammonia, and isobutene natural refrigerants. He studied the effects on COP and optimum area ratio of ejector at different evaporator and condenser temperatures. Sarkar [5] analyzed the same system and refrigerants in another study, but using constant area mixing model. He concluded that the constant area model provided better performance. Bilir and Ersoy [6] executed a similar study on EVCS using constant area model with R134a and additionally considered the effect of secondary flow pressure drop. They concluded that EVCS performed better than a standard VCS even in off-design working situations. Disawas and Wongwises [7] also carried out a similar analysis but with flooded evaporator. The literature shows that the ejector in place of the conventional expansion devices in single evaporator vapor compression systems has the potential; however, the configuration of dual evaporator cycle with ejector still needs to be examined thoroughly.

In a single refrigerator-freezer unit, cooling in the food compartment is made by air circulation from the freezer section and is thus responsible for the non-uniformity of temperature in the food section. Secondly, the freezer temperature lesser than the dew point causes humidity of air in circulation to reduce and it causes fruits and vegetables to lose its freshness in less time. A dual evaporator refrigeration system can maintain the required temperature, air flow rate and humidity in the refrigerator and freezer section independently. The energy saving is also possible with dual evaporator system as the food section refrigeration requires higher evaporator temperature than the freezer section.

Hadi et al. [8] designed a condenser outlet split (COS) configuration using independent ejector vapor compression systems for both the evaporators. They used two compressors to handle the output of two evaporators at different pressures. The improvement of 48.07% in COP was obtained with the modified cycle using R290. Cui Li et al. [9] replaced pressure reducing valve after the high pressure evaporator with a variable area ratio ejector in their COS dual evaporator cycle. The pressure recovery and reduced compression ratio due to the use of ejector improved the system performance. Sarkar [10] compared two configurations of dual evaporator cycle with transcritical CO_2. Lawrence and Elbel [11] also analyzed two configurations; first COS configuration with ejector and second ejector outlet split

(EOS) configuration. They performed experiments with different motive nozzle geometries using R134a. Later they [12] executed experiments on EOS configuration using R1234yf and R134a. Latra et al. [13] also examined the performance of COS cycle with ejector for R134a and R1234yf. Unal and Yilmaz [14] analyzed COS cycle with ejector for a bus air conditioning system. The effect of sub-cooling and the temperatures of condenser and evaporators were highlighted while working with R134a. Joen et al. [15] compared the system in single and dual evaporator modes using R600a. Gao et al. [16] numerically compared COS ejector cycle with a modified cycle having one flooded evaporator and one dry evaporator connected with ejector and separator.

Presently, R134a having global warming potential (GWP) of 1450, is being used extensively mainly in air conditioning industries, but as per the various treaties, this refrigerant is to be discontinued in a phase manner [17]. Researchers have been proposing R1234yf as a substitute of R134a in the existing systems with minor modifications. The refrigerant R1234yf has zero ODP and quite negligible, though not zero GWP. Minor and Spatz [18] examined R1234yf in place of R134a in a portable air-conditioning set up and found that without any notable changes, the COP with R1234yf is only 4–8% lower than R134a. Similar observations have also been conveyed by Zilio et al. [17], Jarall [19] and Navarro-Esbri et al. [20]. The present work includes the comparison analysis of R1234yf with R134a in the ejector assisted dual evaporator system.

The proposed configuration of dual evaporator ejector cooling system had been analyzed by Elakdhar et al. [21] but for the same given cooling capacity in both the evaporators. However, the present work calculates cooling capacity of the evaporators for fixed condenser, evaporator, and condenser temperatures. It also analyzes the effect of dryness fraction at the exit of flooded evaporator. Further an eco-friendly refrigerant R1234yf has been considered in the present analysis and compared with a similar configuration using conventional expansion devices. A quantitative performance comparison has been obtained for R134a, R152a, and R1234yf. The targeted system is a cold storage system in India. Here the climate conditions can vary the condenser temperature in the range of 36 to 44 ℃ depending on the location and month of the year. For a variety of Potato storage, the required temperature may be from 2 to 15 ℃ and it can be achieved with the range of evaporator temperature considered in the present analysis. The constant pressure mixing approach has been adopted for the modeling of ejector. Unit mass flow rate condition of the refrigerant is considered in the present work. The novelty of the system

Sachdeva *et al. Int. J. Air-Cond. Ref.*   *(2023) 31:20*

Page 3 of 16

lies in its configuration, the input parameters and the refrigerant analyzed.

2 System explanation

Figure 1 depicts an ejector assisted dual evaporator cycle (EA-DEC) and Fig. 2 presents the corresponding P–h diagram. The condensed refrigerant at state 3 is expanded to state 4 in a conventional expansion valve-1 and thereafter receives heat in the evaporator-1. The evaporator-1 is a kind of flooded evaporator, so the refrigerant leaves evaporator-1 in mixed phase corresponding to the state point 5. Thereafter, a separator is employed to get the liquid and the vapor part at constant pressure. The liquid refrigerant at state 7 is expanded to state 8 in the expansion valve-2 and the process 8 to 9 happens in the evaporator-2 which is a dry evaporator. On the other side, the vapor refrigerant exiting the separator at state 6 is expanded to state point 10 in the primary nozzle of ejector and creates pressure lower than the pressure of evaporator-2.

Consequently, the ejector sucks the vapor refrigerant exiting from the evaporator-2 at state 9. At constant pressure corresponding to state 10, mixing of these two fluids takes place. The diffusor of ejector increases the pressure of mixed refrigerant corresponding to state 1 and then compressor increases the pressure further up-to the condenser pressure. The latent heat is taken away by the condenser and the cycle works. The saturated refrigerant in vapor and liquid phase exiting from the separator are known as primary and secondary refrigerant respectively.

Figure 3 is a schematic diagram of a conventional multi expansion dual evaporator cycle (ME-DEC) and Fig. 4 is the corresponding P–h chart. The only difference in this configuration is the use of a pressure reducing valve instead of ejector after the separator. The pressure reducing valve drops pressure of the vapor refrigerant exiting from the separator to the pressure of evaporator-2, hence the total refrigerant is supplied to the compressor at the evaporator-2 pressure. Rest of the cycle is same as EA-DEC.

3 Methodology

Following simplifications have been considered to in the study:

1. The refrigerant exists at saturated vapor state and saturated liquid state at the outlets of evaporator-2 and condenser respectively.
2. Liquid and vapor leave the separator at saturated states corresponding to the pressure in separator.
3. The velocity at the inlet of primary nozzle and the outlet of diffuser is negligible.
4. Pressure of secondary fluid at the primary nozzle outlet is same as the pressure of primary fluid.
5. The motive nozzle, suction and mixing section, and diffuser have a fixed efficiency.
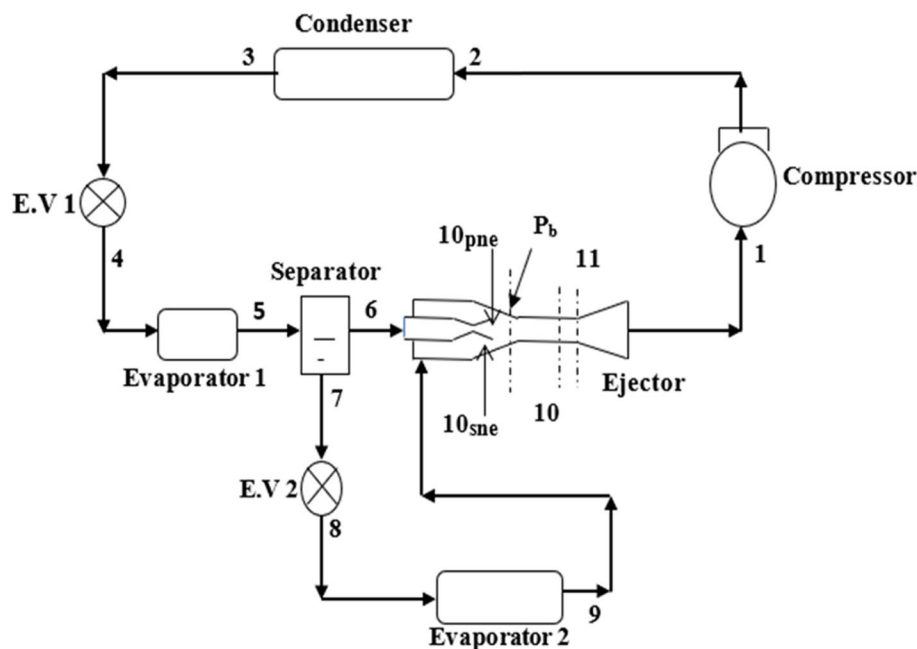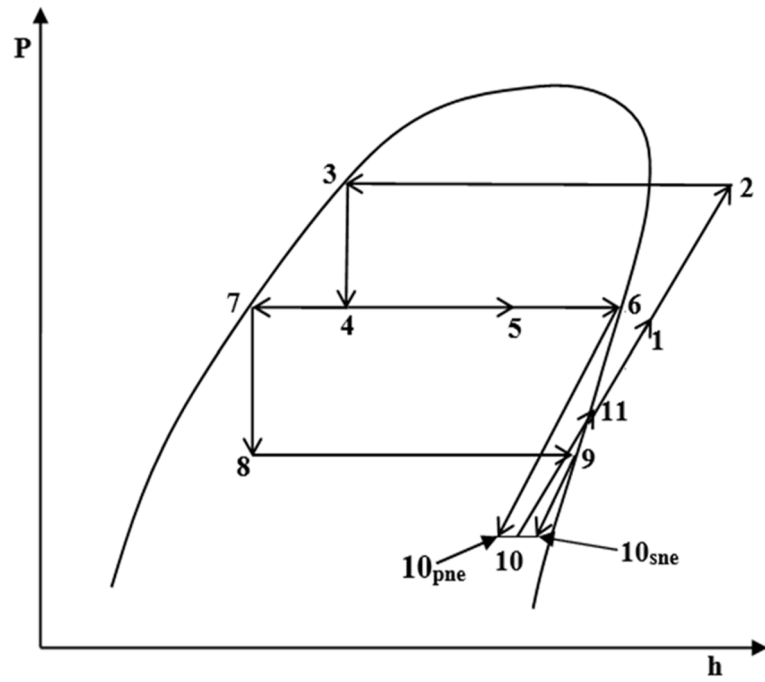

Fig. 1 EA-DEC configuration
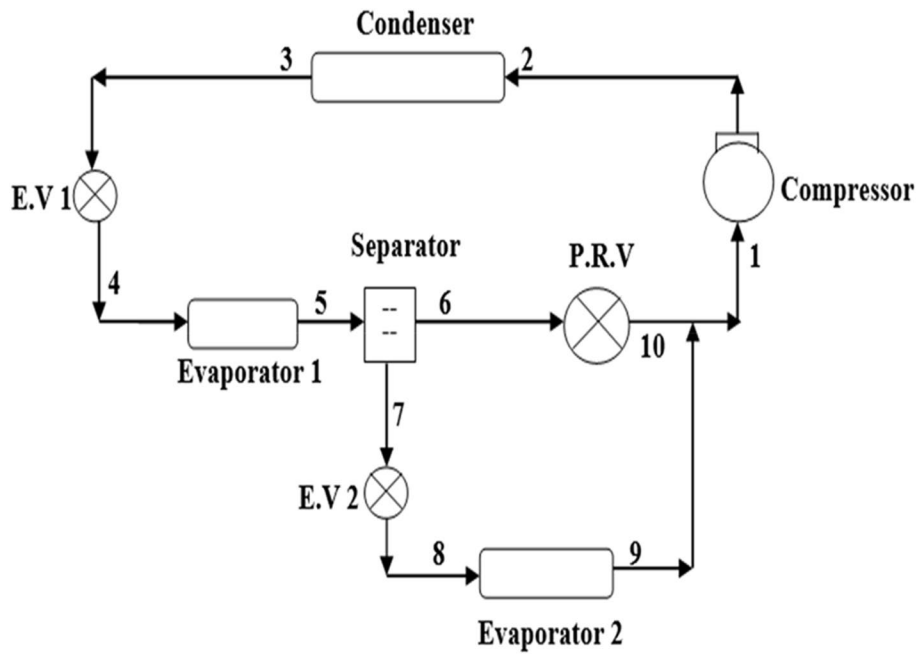
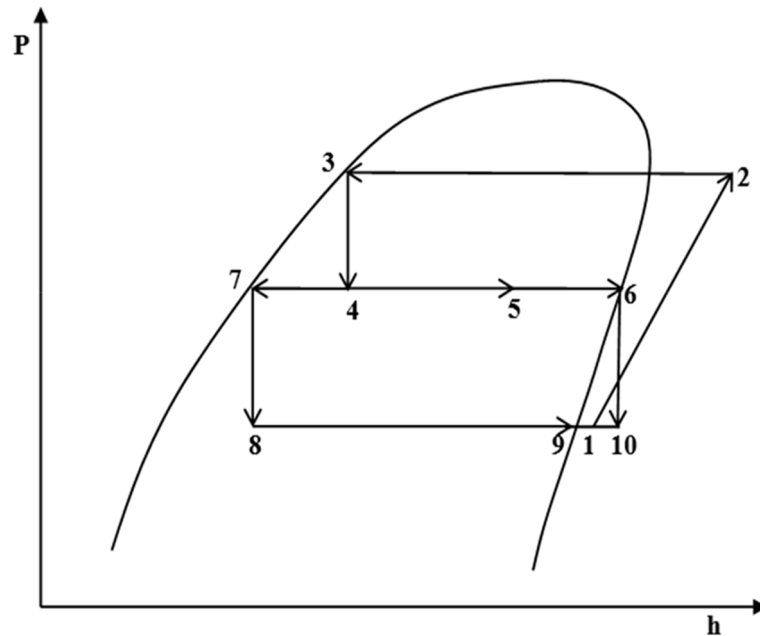**Fig. 2** P–h chart of EA-DEC

Fig. 3 Schematic of ME-DEC

Fig. 4 P–h diagram of ME-DEC

6. Pressure drop in condenser, separator, evaporator, and the connecting conduits is neglected.
7. There is no heat loss in the system.
8. Any friction loss in the constant area section is ignored.

Thermodynamic modelling includes mass, energy, and entropy balance in the condenser and evaporator of the system. The equations employed for the ejector being complex are only explained as under.

3.1 Ejector

3.1.1 Primary refrigerant flow in the motive nozzle

The velocity of primary fluid at nozzle exit (u_{10pne}) is calculated using equation as under:

$$u_{10pne} = \sqrt{2 * \eta_{pn}(h_6 - h_{10pne,is})} \qquad (1)$$

The isentropic efficiency of nozzle η_{pn} is stated as below:

$$\eta_{pn} = \frac{h_6 - h_{10pne}}{h_6 - h_{10pne,is}} \qquad (2)$$

The actual enthalpy at the outlet of primary nozzle is determined using efficiency as under:

$$h_{10pne} = h_6 - \eta_{pn} * (h_6 - h_{10pne,is}) \qquad (3)$$

The Mach number at the outlet of primary nozzle, i.e., state point 10pne is calculated taking ideal gas behavior

as provided by El-Dessouky et al. [22] Pridasawas [23] and Sun and Eames [24].

$$M_{10pne} = \sqrt{\frac{2 * \eta_{pn}}{\gamma - 1}\left[\left(\frac{P_5}{P_b}\right)^{\left(\gamma - \frac{1}{\gamma}\right)} - 1\right]} \qquad (4)$$

Area of primary nozzle exit is calculated by the equation as under

$$a_{10pne} = \frac{\dot{m}_p}{\rho_{10pne} * u_{10pne}} \qquad (5)$$

where $\dot{m}_p$ is the mass flow rate of vapor or motive refrigerant and is calculated by

$$\dot{m}_p = x_5 * \dot{m} \qquad (6)$$

3.1.2 Secondary refrigerant flow in the secondary nozzle

Similarly, for the secondary refrigerant flow in the imaginary secondary nozzle, the velocity at the nozzle outlet is obtained by

$$u_{10sne} = \sqrt{2 * (h_9 - h_{10sne,is})} \qquad (7)$$

The pressure at the exit of secondary nozzle is considered to be same as it is at the outlet of primary nozzle. This pressure is also named as back pressure. It is assumed initially and then iterated to the correct one in the code written in Engineering Equation Solver (EES) [25].

Likewise, the Mach number of secondary fluid at the secondary nozzle outlet (under ideal gas) is calculated using equation given in [23]:

$$M_{10sne} = \sqrt{\frac{2}{\gamma - 1}\left[\left(\frac{P_9}{P_b}\right)^{\left(\gamma - \frac{1}{\gamma}\right)} - 1\right]} \qquad (8)$$

Area of secondary nozzle outlet is calculated using equation as under

$$a_{10sne} = \frac{\dot{m}_s}{\rho_{10sne} * u_{10sne}} \qquad (9)$$

where $\dot{m}_s$ is the mass flow rate of vapor or secondary refrigerant and calculated as

$$\dot{m}_s = (1 - x_5) * \dot{m} \qquad (10)$$

3.1.3 Mixing of primary and secondary fluid before shock
Momentum balance of the ideal mixing process is made to find velocity of the mixed fluid

$$u_{10i} = \frac{u_{10pne} + \mu * u_{10sne}}{1 + \mu} \qquad (11)$$

The ratio of mass flow rates of secondary fluid to primary fluid is the entrainment ratio μ (ER) of ejector.

$$\mu = \frac{\dot{m}_s}{\dot{m}_p} \qquad (12)$$

The entrainment ratio gets fixed due to the pre-defined dryness fraction at state 5 and mass flow rate ($\dot{m}$) of the total refrigerant as unit, i.e., 1.0 kg/s; therefore, the ejector has been designed for a fixed ER.

Total area of mixing section is calculated as:

$$a = a_{10pne} + a_{10sne} \qquad (13)$$

The actual velocity of the mixed fluid is determined using mixing efficiency η_m as provided by Yu et al. [26]

$$u_{10a} = \sqrt{\eta_m} * u_{10i} \qquad (14)$$

The enthalpy h_{10} of the mixed fluid is obtained by doing the energy balance

$$h_{10} = \frac{h_6 + \mu h_9}{1 + \mu} - \frac{(u_{10a})^2}{2} \qquad (15)$$

$$\dot{m}_n = \rho_{10} * u_{10a} * a \qquad (16)$$

where $\dot{m}_n$ is the new calculated mass flow rate that is compared with the assumed mass flow rate and iterated till the desired back pressure is achieved.

The critical Mach numbers of primary and secondary fluids at the respective nozzle exits are found using the equations as in [22]

$$M_{10pne,c} = \sqrt{\frac{M_{10pne}{}^2(\gamma + 1)}{M_{10pne}{}^2(\gamma - 1) + 2}} \qquad (17)$$

$$M_{10sne,c} = \sqrt{\frac{M_{10sne}{}^2(\gamma + 1)}{M_{10sne}{}^2(\gamma - 1) + 2}} \qquad (18)$$

The critical Mach number at state 10 in terms of the critical Mach numbers of primary and secondary fluids at their nozzle exits is obtained as under [26].

$$M_{10,c} = \sqrt{\eta_m} * \left[\frac{M_{10pne,c} + \mu * M_{10sne,c}\sqrt{T_{e2}/T_{e1}}}{\sqrt{(1 + \mu)(1 + \mu * (T_{e2}/T_{e1}))}}\right] \qquad (19)$$

The Mach number of mixed fluid is obtained using the relation with critical Mach number

$$M_{10} = \sqrt{\frac{2M_{10,c}{}^2}{(\gamma + 1) - M_{10,c}{}^2(\gamma - 1)}} \qquad (20)$$

3.1.4 Consideration of normal shock wave
The normal shock alters the flow to subsonic; subsequently increases the pressure of fluid. The Mach number and the pressure of fluid after the shock at point 11 are found using below equations [26]:

$$M_{11} = \sqrt{\frac{M_{10}{}^2 + 2/(\gamma - 1)}{2\gamma * \frac{M_{10}{}^2}{\gamma - 1} - 1}} \qquad (21)$$

$$\frac{P_{11}}{P_{10}} = \frac{1 + \gamma * M_{10}{}^2}{1 + \gamma * M_{11}{}^2} \qquad (22)$$

3.1.5 Fluid flow in the diffuser

$$\frac{P_1}{P_{11}} = \left[\frac{(\gamma - 1)M_{11}{}^2 + 1}{2}\right]^{\frac{\gamma}{\gamma - 1}} \qquad (23)$$

The velocity of fluid leaving the ejector is ignored and in this way the enthalpy at ejector exit is obtained [25]:

$$h_1 = h_{10} + \frac{h_{11is} - h_{10}}{\eta_d} \qquad (24)$$

Using diffuser efficiency η_d, actual enthalpy of the fluid is obtained by

Sachdeva *et al. Int. J. Air-Cond. Ref.*   (2023) 31:20

Page 7 of 16

$$\eta_d = \frac{h_{1is} - h_{10}}{h_1 - h_{10}} \tag{25}$$

Pressure lift ratio is the ratio of the ejector exit pressure (p_{11}) to the secondary fluid inlet pressure (p_9).

$$PLR = \frac{P_{11}}{P_9} \tag{26}$$

The COP of cycle is found as under.

$$COP = \frac{\dot{Q}}{\dot{W}_{comp}} \tag{27}$$

4 Model validation

Sarkar [27] has considered almost similar cycle but with additional separator after the ejector with CO_2 refrigerant. The liquid part separated by the second separator was expanded and supplied to the evaporator-2 and the saturated vapor was supplied to the compressor.

In the present configuration, there is no need of the second separator as the refrigerant after coming out of the ejector exists in vapor phase only. In the proposed configuration, ejector employed is of single phase ejector which is same as in the generator based refrigeration system of Chen et al. [28]. The present code has been modified for refrigerant R123 and the operating conditions as considered by Chen et. al. [28]. Figure 5 shows that the results are in good agreement.

Figure 6 shows flow chart of the model made in EES.

To provide more confidence in the results, the EA-DEC is altered to a single evaporator ejector refrigeration system and validated with Huashan Li et al. [29] for the refrigerant R1234yf at the evaporator temperature of 5 °C and condenser temperature of 40 °C, while varying the secondary pressure drop (SNDP) from 0

to 50 kPa. The efficiency of nozzles, mixing, and diffuser sections of the ejector are kept same as in [29]. The COP obtained is in agreement with [29] as shown in Table 1.

5 Results and discussion

The EA-DEC is numerically analyzed in Engineering Equation Solver (EES) for the fluids R134a, R152a, and R1234yf at the designed conditions as shown in Table 2. The various efficiencies of ejector are taken from the reference [28].

The yielded properties and various mass flow rates of EA-DEC at various state points as obtained using the model for R152a are shown in Table 3.

The important performance parameters provided by the model at the designed conditions are mentioned in Table 4. The temperatures of evaporator-1, evaporator-2 and condenser, dryness fraction after evaporator-1, and the total mass flow rate of refrigerant are kept same in both the cycles, i.e., EA-DEC and ME-DEC for the true comparison. Being fixed dryness fraction and unit total mass flow rate of the refrigerant, the liquid mass flow rate towards evaporator-2 also got fixed. Consequently, same cooling capacity is obtained in both the evaporators of both the systems. In case of EA-DEC, the entrainment ratio also gets fixed due to fixed primary and secondary mass flow rates of the refrigerant. Therefore, the comparison of both the cycles truly advocates the advantages of ejector in dual evaporator cycle. Table 4 clearly shows that for the same cooling capacity at same operating temperatures, compressor work required in EA-DEC is lesser than that of ME-DEC. The COP of EA-DEC is 16.78%, 17.84%, and 18.83% higher than that of ME-DEC with R134a, R152a, and R1234yf respectively. Further, it is found that the COP obtained with R152a is the
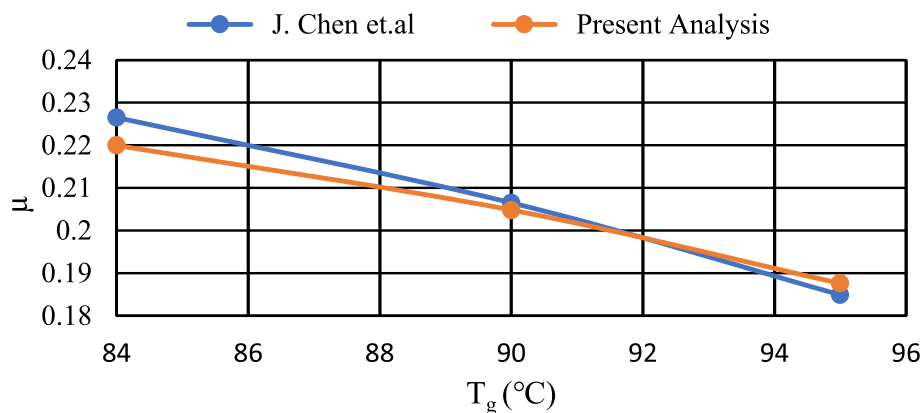

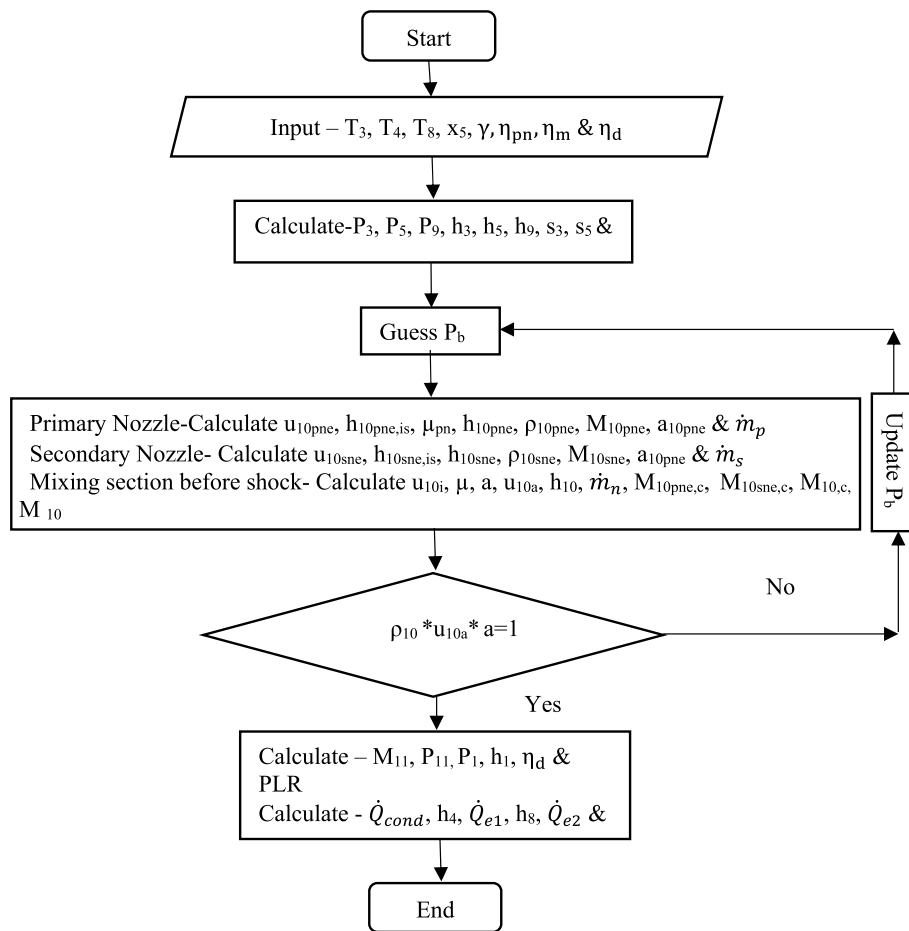**Fig. 5** Validation of the ejector model with Chen et al. [28]

Sachdeva *et al. Int. J. Air-Cond. Ref.*   (2023) 31:20

Page 8 of 16

Fig. 6 Flow diagram

Table 1 Validation with Huashan Li et al. [29]

S.No.	SNDP(ΔP) kPa	Present Model COP	Huashan Li et al. [29] COP	Error (%)
1	0	5.752	5.791	.673
2	5	5.889	5.884	.085
3	10	5.918	5.902	.270
4	15	5.925	5.905	.340
5	20	5.920	5.889	.530
6	25	5.902	5.881	.360
7	30	5.889	5.868	.360
8	35	5.866	5.855	.190
9	40	5.842	5.819	.390
10	45	5.816	5.792	.410
11	50	5.788	5.763	.430

Table 2 Designed conditions

Input parameters	Values
Condenser temperature (T_c in ℃)	40
Evaporator-1 temperature (T_{e1} in ℃)	10
Evaporator-2 temperature (T_{e2} in ℃)	−6
Primary nozzle efficiency (η_{pn} in %)	95
Diffuser efficiency (η_d in %)	95
Mixing section efficiency (η_m in %)	95
Dryness fraction after evaporator-1 (x_5)	0.7
Total mass flow rate of the refrigerant (kg/s)	1.0

highest and R1234yf is the lowest. The compressor work and cooling capacity with R152 are 45% and 76% higher respectively than that of R1234yf.

5.1 Effects of condenser temperature variation
5.1.1 *Compressor work with the condenser temperature variation*

Figure 7 depicts that the compressor work requirement enhances with the uplift in condenser temperature. The trend is obvious as the rise in condenser temperature

Sachdeva *et al. Int. J. Air-Cond. Ref.*   (2023) 31:20

Page 9 of 16

Table 3 Thermodynamic properties at various state points for R152a

State point	T($^\circ$C)	P (kPa)	m (kg/s)	h (kJ/kg)	s (kJ/kg-K)
1	4.925	285.2	1	511.2	2.131
2	53.64	910.3	1	550.3	2.131
3	40	910.3	1	271.7	1.242
4	10	373.3	1	271.7	1.254
5	10	373.3	1	424.5	1.793
6	10	373.3	0.7	513.3	2.107
7	10	373.3	0.3	217.3	1.062
8	−6	211.9	0.3	217.3	1.065
9	−6	211.9	0.3	502.4	2.133
10_{pne}	−17.08	136.6	0.7	482.4	2.107
10_{sne}	−17.08	136.6	0.3	489	2.133
10	−17.08	136.6	1	488.5	2.131
11	−10.36	179.2	1	511.2	2.131

Table 4 Performance parameters at the designed conditions

Parameters	R152a	R134a	R1234yf
μ	0.43	0.43	0.43
PLR	1.346	1.345	1.327
W_{EA} (kJ/s)	39.02	24.76	19.85
W_{ME} (kJ/s)	50.22	31.78	25.67
$\dot{Q}_{e1}$ (kJ/s)	152.7	90.68	68.67
$\dot{Q}_{e2}$ (kJ/s)	85.55	54.44	44.12
$\dot{Q}_{e\ total}$ (kJ/s)	238.3	145.1	112.8
COP_{EA}	6.106	5.862	5.682
COP_{ME}	4.744	4.567	4.394

improves pressure ratio of compressor and thus compressor work.

Figure 7 shows that for the considered range of condenser temperature, the compressor work is higher in ME-DEC in comparison to EA-DEC for all the three refrigerants. At condenser temperature 44 °C, the compressor work is higher by 26.58%, 24.08%, and 27.26% for the fluids R152a, R134a, and R1234yf respectively. However, the percentage increase in compressor work in EA-DEC is higher than ME-DEC and it is 16.71% and 21.1% in ME-DEC and EA-DEC respectively with R152a for the condenser temperature variation from 36 °C to 44 °C. Similarly, it is 16.09% and 20.3% for R134a and 15.55% and 19.8% R1234yf.

5.1.2 Cooling effect with the condenser temperature variation

The enthalpy at state point 4 is determined to augment with the rise in condenser temperature; however, as the dryness fraction at state 5 is fixed as mentioned in Table 1; therefore, the enthalpy difference between state 4 and 5 is decreased and thus the cooling capacity in the evaporator-1 is reduced as shown in Fig. 8. The mass flow rate of refrigerant in evaporator-2 depends on the dryness fraction at state 5, which is fixed, thus the cooling effect in evaporator-2 is not a function of condenser temperature for the considered configuration. Both the systems have been compared for the same cooling capacity. Total cooling capacity is decreased by 6.18%, 7.94%, and 9.86% for the working fluids R152a, R134a, and R1234yf respectively at 44 °C.
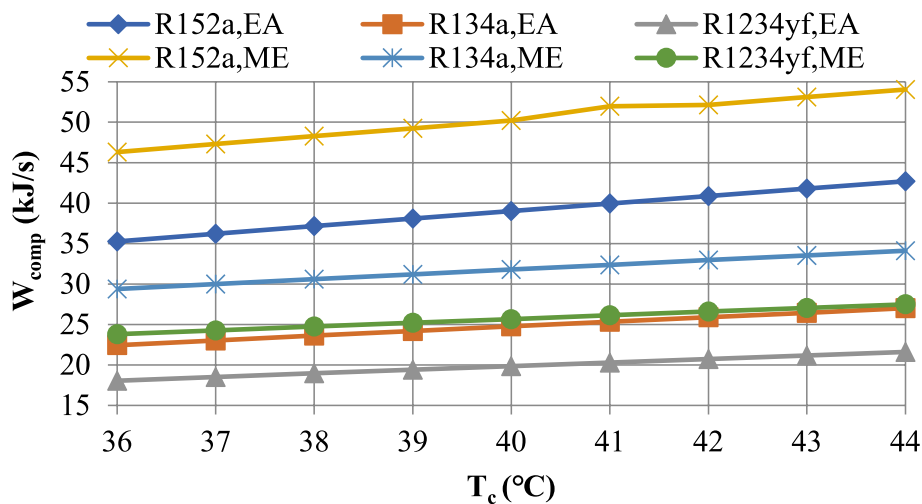

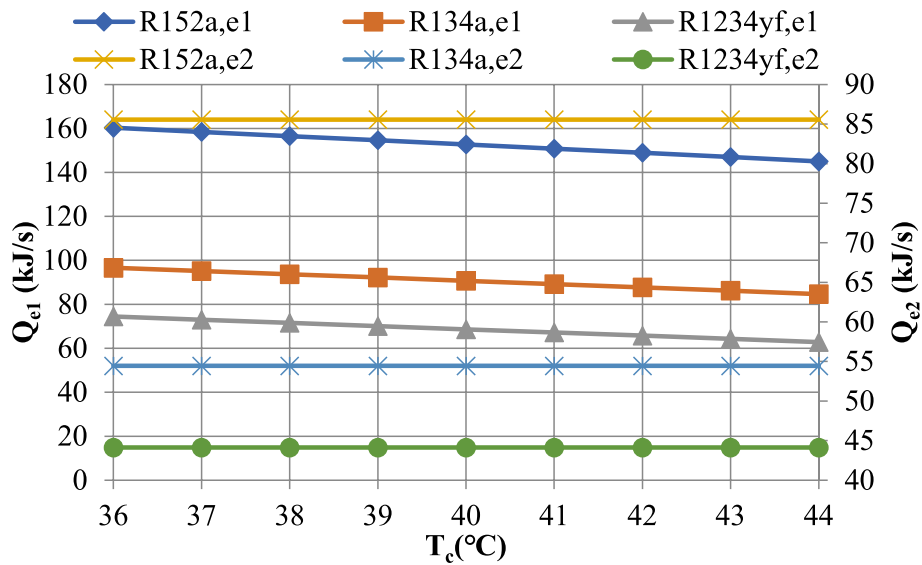**Fig. 7** Compressor work with condenser temperature

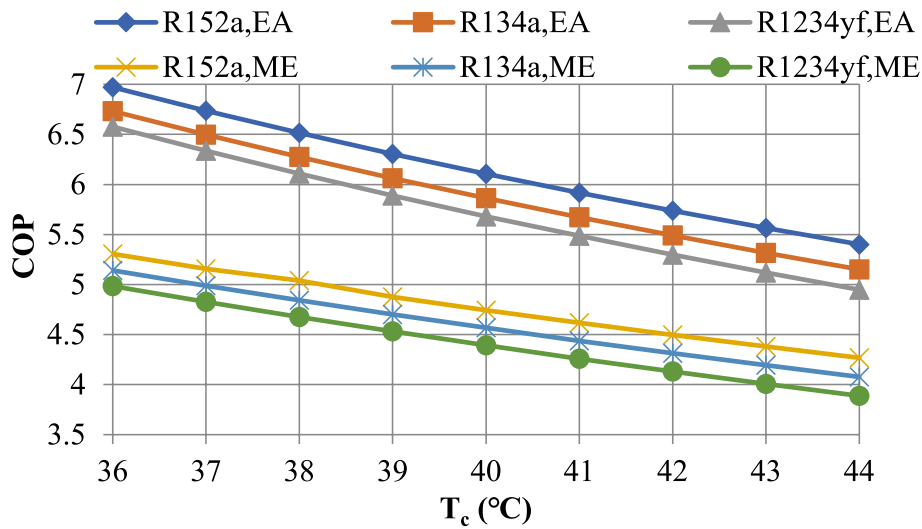**Fig. 8** Cooling capacity with condenser temperature

Fig. 9 COP with condenser temperature

5.1.3 Coefficient of performance with the condenser temperature variation

The rise in condenser temperature enhances compressor work and reduces cooling capacity in both the systems as discussed.

Figure 9 shows that the rate of decrease of COP is more in EA-DEC than ME-DEC for all the refrigerants but still the COP in EA-DEC is higher even at high condenser temperatures. The COP improvement is decreased by 22.52%, 23.48%, and 24.77% for R152a, R134a, and R1234yf respectively with the rise in condenser temperature from 36 °C to 44 °C in EA-DEC.

5.2 Effects of evaporator-1 temperature variation

5.2.1 Compressor work with the evaporator-1 temperature variation

The enthalpy of saturated vapor gets slightly increased for the refrigerants with the increase in saturation temperature. Therefore, the enthalpy after pressure reducing valve is a bit higher which in turn increased the degree of superheat before the compression process in case of ME-DEC. For the same pressure ratio, the compressor work is actually increased, though negligible, for R152a, R134a and R1234yf as shown in Fig. 10. On the other side, the pressure of motive fluid
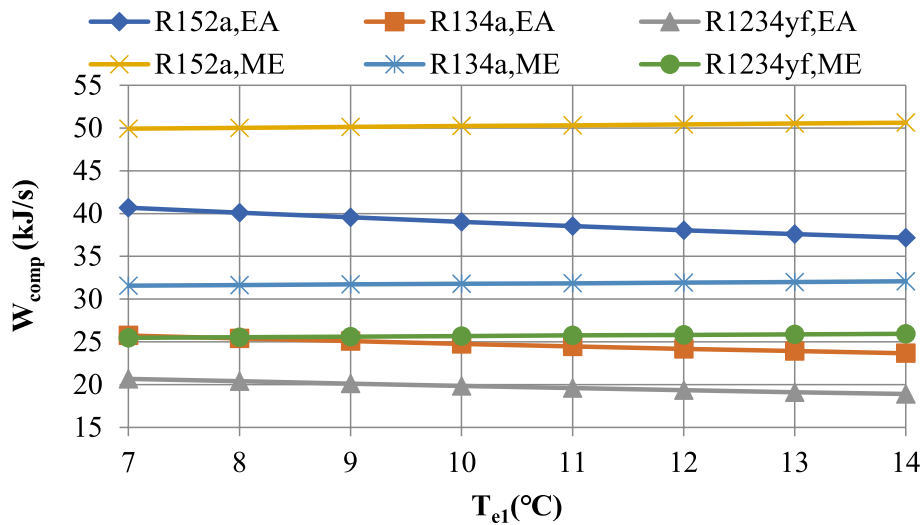
Fig. 10 Compressor work with evaporator-1 temperature

is enhanced with the rise in evaporator-1 temperature, which in turn increased the pressure at the exit of ejector. Therefore, the pressure ratio of compressor is decreased and thus it reduced the compressor work in EA-DEC. The compressor work is reduced by 8.63%, 8.08%, and 8.56% with R152a, R134a, and R1234yf respectively while changing the evaporator-1 temperature from 7 °C to 14 °C.

5.2.2 Cooling effect with the evaporator-1 temperature variation

The enthalpy at state 5 is found to increase at high saturation temperatures for the fixed dryness fraction x_5, which in turn increased the enthalpy difference (h_4-h_5)

and thus cooling effect in the evaporator-1. However, the cooling effect in evaporator-2 is decreased, because the enthalpy at state 8 is more after expansion from high pressure of separator. It enthalpy difference (h_8-h_9) is thus decreased and so the cooling capacity as shown in Fig. 11.

The cooling effect in evaporator-1 is increased by 4.54%, 6.35%, and 8.87% with the rise in evaporator-1 temperature from 7 °C to 14 °C for R152a, R134a, and R1234yf respectively. Further, it is decreased by 4.21%, 5.19%, and 6.11% in evaporator-2 with R152a, R134a, and R1234yf respectively for the considered temperature range. Overall, there is a little increase in the total cooling capacity.
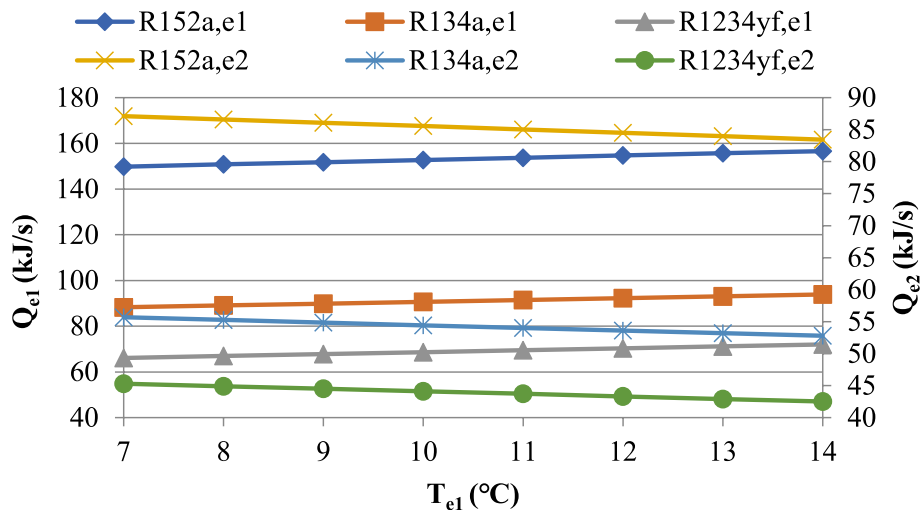

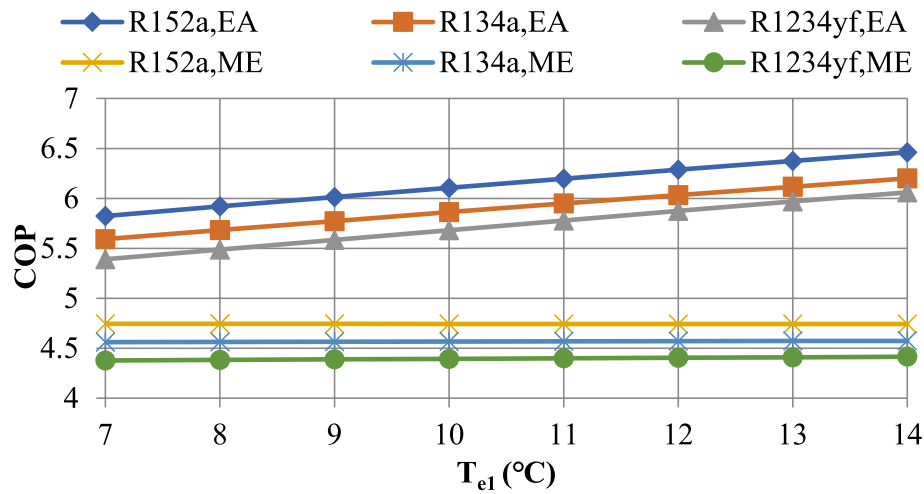**Fig. 11** Cooling effect with evaporator-1 temperature

Fig. 12 COP with evaporator-1 temperature

5.2.3 Coefficient of performance with the evaporator-1 temperature variation

The total cooling capacity is increased a bit and the compressor work is almost constant in case of ME-DEC as the evaporator-1 temperature is raised; therefore, the COP is found to increase slightly. However, the variation in COP is less than 3.5% as shown in Fig. 12. The compressor work in case of EA-DEC is reduced with the rise in evaporator-1 temperature and cooling effect is also increased marginally, thus COP increases considerably. Figure 12 shows that the COP of EA-DEC cycle is increased by 10.9%, 10.87%, and 12.42% with the change in evaporator-1 temperature from 7 °C to 14 °C for R152a, R134a, and R1234yf respectively.

5.3 Effects of evaporator-2 temperature variation

5.3.1 Compressor work with the evaporator-2 temperature variation

The pressure ratio of compressor decreases in ME-DEC as the suction needs to take place at high pressure with the rise in evaporator-2 temperature; therefore, the compressor work is decreased as shown in Fig. 13. However, the pressure at the outlet of ejector is increased due to the increase in secondary fluid, i.e., evaporator-2 pressure in EA-DEC. It decreased the pressure ratio and thus the compressor work. The compressor work is reduced by 12.18%, 12.56%, and 11.69% with R152a, R134a, and R1234yf respectively in EA-DEC and it is 18.08%, 18.05%, and 17.93% with R152a, R134a, and R1234yf respectively in ME-DEC.
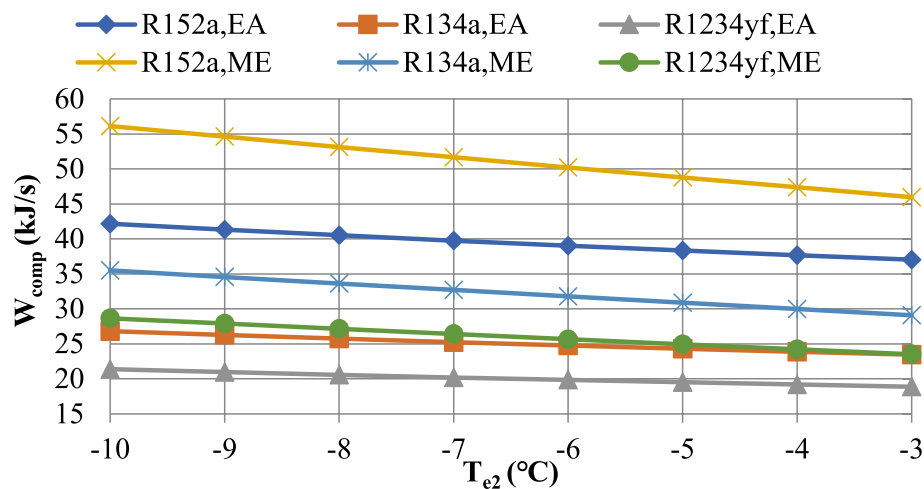

Fig. 13 Compressor work with evaporator-2 temperature

5.3.2 Cooling effect with the evaporator-2 temperature variation

The cooling effect in evaporator-1 is independent of evaporator-2 temperature; therefore, it is same as it is at the designed conditions. However, there is a bit increase in the cooling effect of evaporator-2 with the rise in its temperature as the enthalpy of saturated liquid is decreased at higher temperature, which in turn decreased the specific enthalpy difference. Fundamentally total refrigeration effect is decreased, but in real, the effect is very little as shown in Fig. 14.

5.3.3 Coefficient of performance with the evaporator-2 temperature variation

The total cooling effect remains almost constant and the compressor work decreases; therefore, COP of both the systems is enhanced with the rise in evaporator-2 temperature.

Figure 15 shows that the COP of EA-DEC cycle is increased by 14.58%, 15.38%, and 14.65% with the rise in evaporator-2 temperature from -10 °C to -3 °C for R152a, R134a, and R1234yf respectively. It is 22.81%, 23.11% and 23.36% for R152a, R134a, and R1234yf respectively in ME-DEC.

5.4 Effects of dryness fraction (x_5) variation
5.4.1 Compressor work with the dryness fraction (x_5) variation

There is no effect of dryness fraction at state 5, i.e., x_5 on compressor work as the mass flow rate and inlet and outlet conditions for the compressor are independent to this variable in case of ME-DEC. However, in EA-DEC, the primary fluid flow rate is increased with the increase in
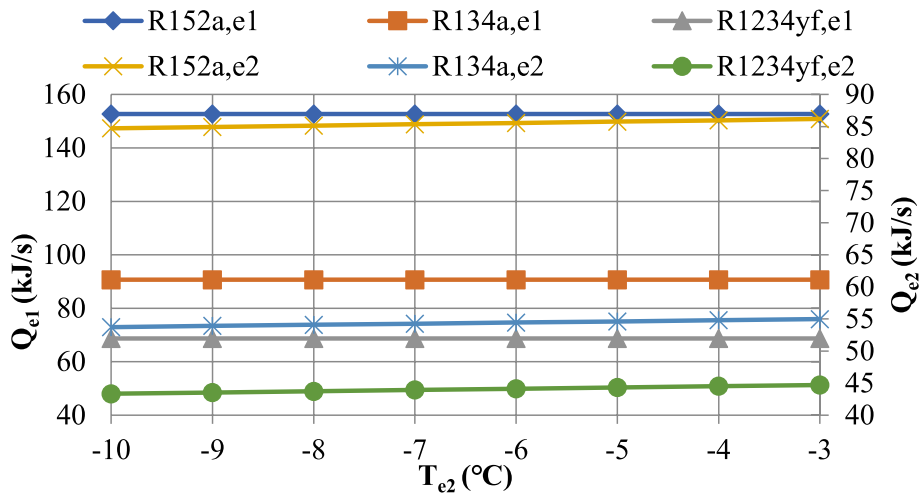

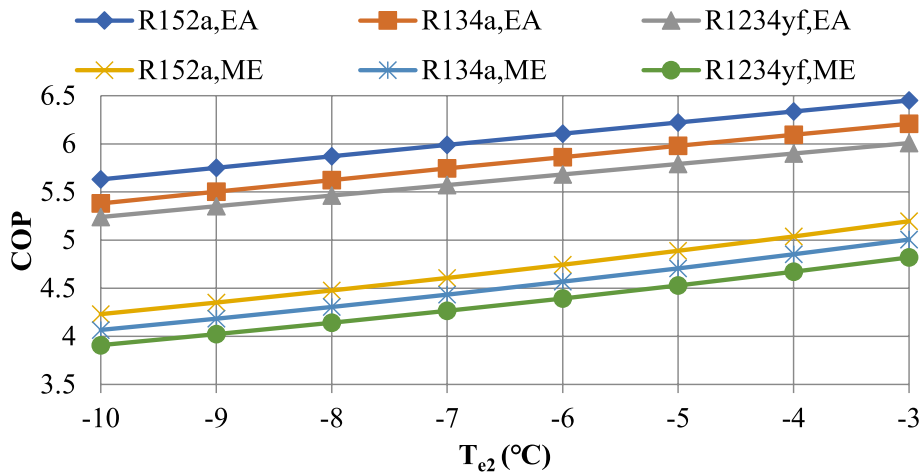**Fig. 14** Cooling capacity with evaporator-2 temperature
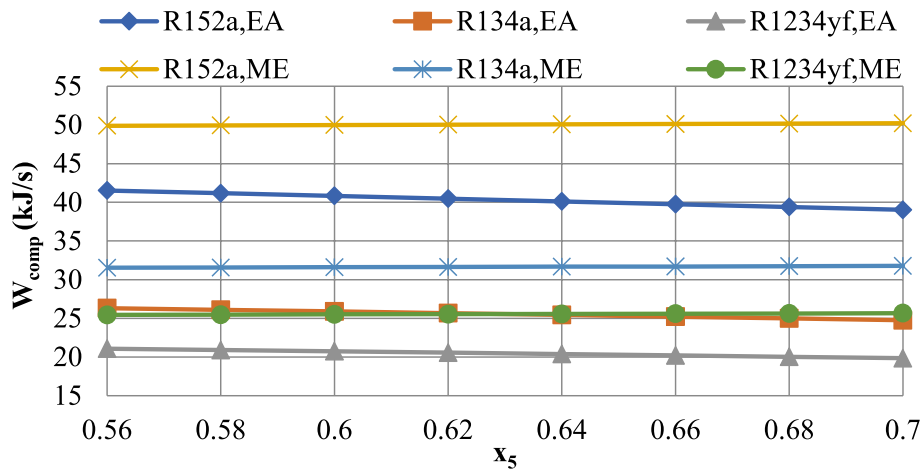

Fig. 15 COP with evaporator-2 temperature

Fig. 16 Compressor work with dryness fraction x_5

x_5 and thus it increased the exit pressure of ejector. The increase in suction pressure lowered the pressure ratio of compressor which in turn reduced the work of EA-DEC. Figure 16 shows that the compressor work of EA-DEC is decreased by 6.02%, 5.92%, and 5.83% with the increase in dryness fraction from 0.56 to 0.70 for R152a, R134a, and R1234yf respectively.

5.4.2 Cooling capacity with the dryness fraction (x_5) variation

The primary fluid mass flow rate in evaporator-1 is found to increase but it is decreased in evaporator-2 with the rise in dryness fraction at state 5. Also the specific enthalpy difference of the working fluid flowing in evaporator-1 is increased with this change in x_5. Figure 17 depicts that the cooling effect in evaporator-1 is increased by 37.19%, 41.73%, and 47.26% but in evaporator-2 it is decreased by 31.83%, 31.82%, and 31.81% with the increase in dryness fraction. However, total cooling capacity of the systems increases marginally.

5.4.3 Coefficient of performance with the dryness fraction (x_5) variation

There is a bit increase in the total cooling effect, and the compressor work is almost constant in case of ME-DEC; therefore, the COP change is negligible. It is less than 3.5% for the dryness fraction range at state 5 from 0.56 to 0.7 as shown in Fig. 18.

The compressor work in case of EA-DEC is decreased and cooling capacity is increased, thus the COP is enhanced with the rise in dryness fraction. Figure 18 shows that the COP of EA-DEC cycle is increased by 7.06%, 7.28%, and 7.55% with the dryness fraction from 0.56 to 0.70 for R152a, R134a, and R1234yf respectively.

6 Conclusions

Numerical investigation of an ejector assisted dual evaporator cycle (EA-DEC) has been compared with a similar dual evaporator cycle employing a pressure reducing valve (ME-DEC). The analysis has been executed for
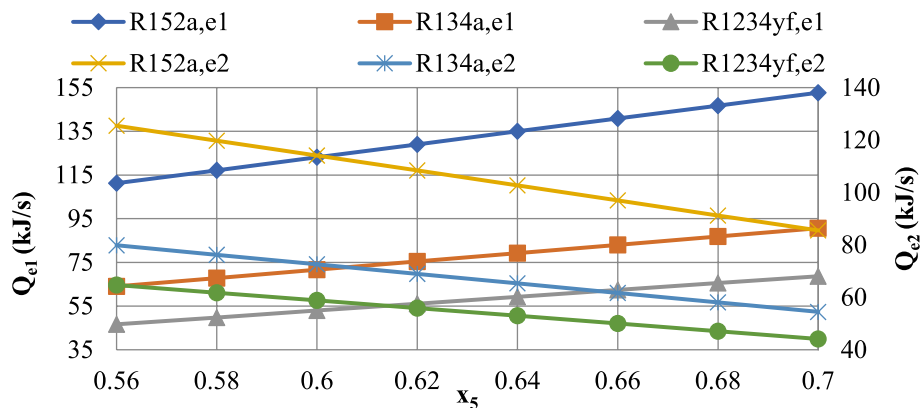

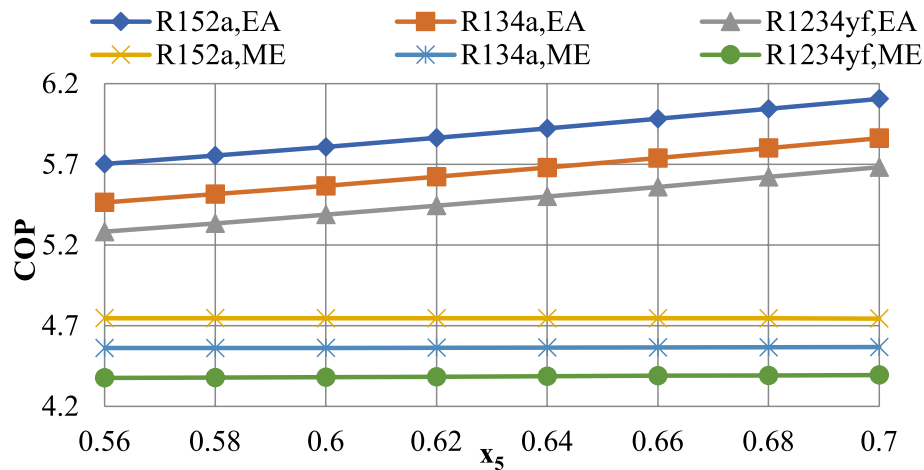**Fig. 17** Cooling capacity with the dryness fraction at state 5

Fig. 18 COP with the dryness fraction at state 5

R152a, R134a, and R1234yf refrigerants. Some of the important conclusions are mentioned as under:

1. The compressor work required for ME-DEC is much higher than that for EA-DEC for the complete range of condenser temperature, though the rate of increase of compressor work with condenser temperature is higher for EA-DEC with all the three refrigerants. For the refrigerant R1234yf, the compressor work is higher by 27.26% in ME-DEC than EA-DEC at 44 ℃, even though the average percentage value of the increase in compressor work is 15.55% in ME-DEC but 19.8% in EA-DEC.

2. The rate of decrease of COP is more in EA-DEC than ME-DEC for all the refrigerants but still the COP is higher in EA-DEC even at high condenser temperature. The COP improvement is decreased by 24.77% and 21.98% with the rise in condenser temperature from 36 ℃ to 44 ℃ in EA-DEC and ME-DEC respectively for the refrigerant R1234yf.

3. The cooling effect in high temperature evaporator is increased, but it is decreased in low temperature evaporator with the rise in high temperature evaporator temperature. The cooling capacity increase is 6.35% and 8.87% in evaporator-1 but the decrease is 5.19% and 6.11% in evaporator-2 with R134a and R1234yf respectively for the rise in evaporator-1 temperature from 7 ℃ to 14 ℃, thus overall there is a little increase in cooling effect of the systems.

4. The compressor work reduction is 12.56% and 11.69% in EA-DEC but 18.05% and 17.93% in ME-DEC with R134a and R1234yf respectively with the decrease in low temperature evaporator temperature from − 3 ℃ to − 10 ℃. The compressor work is much lower than that required in ME-DEC; however, the

rate of decrease in compressor work is comparatively lower in EA-DEC.

5. The compressor work of EA-DEC is found to decrease by 6.02%, 5.92%, and 5.83% with the increase in dryness fraction at the exit of the high temperature flooded evaporator from 0.56 to 0.70 for R152a, R134a, and R1234yf respectively, but there is no change in the compressor work of ME-DEC. The cooling capacity of high temperature evaporator is increased, but that of low temperature evaporator is decreased and overall total cooling capacity of the systems is increased marginally.

7 Nomenclature

EA-DEC Ejector assisted dual evaporator cycle
ME-DEC Multiple expansion dual evaporator cycle
x Dryness fraction
h Enthalpy (kJ/s)
T Temperature (℃)
P Pressure (kPa)
$\dot{m}$ Mass flow rate (kg/s)
a Area (m^2)
u Velocity (m/s)
M Mach Number
$\dot{Q}_e$ Cooling capacity rate (kJ/s)
$\dot{W}$ Work (kJ/s)
COP Coefficient of performance
SNDP Secondary fluid pressure drop

7.1 Symbols

η Efficiency
μ Entrainment ratio
ρ Density (kg/m^3)

Sachdeva *et al. Int. J. Air-Cond. Ref.*   (2023) 31:20

Page 16 of 16

7.2 Subscript

b Back
e Evaporator
e1 Evaporator-1
e2 Evaporator-2
p_n Primary nozzle`
s_n Secondary nozzle
comp Compressor
EA Ejector assisted
ME Multiple expansion

Authors' contributions

Gulshan Sachdeva: Overall guidance, Model develoment and paper writing. Ajay Jaiswar: Results and model validation. Parinam Anuradha: Graphs plotting and Analysis. Vaibhav Jain: Paper correspondance, EES programming, result compilation.

Availability of data and materials

The data that support the findings of this study are available from the corresponding author, [V. Jain], upon reasonable request.

Declarations

Competing interests

The authors declare that they have no competing interests.

References

1. Robinson, D. M., & Groll, E. A. (1998). Efficiencies of transcritical CO_2 cycles with and without an expansion turbine. *International Journal of Refrigeration, 21*(7), 577–589.
2. Kornhauser, A. A. (1990). *The use of an ejector as a refrigerant expander* (pp. 10–19). Proceedings of the 1990 USNCR/IIR-Purdue Refrigeration Conference.
3. Menegay, P., & Kornhauser, A. A. (1996). *Improvements to the ejector expansion refrigeration cycle. Proceedings of the 31st Intersociety Energy Conversion Engineering Conference* (pp. 702–706).
4. Sarkar, J. (2009). Performance characteristics of natural- refrigerants based ejector expansion refrigeration cycles. *Proceedings of IMechE, Part A, Journal of Power and Energy, 223*(5), 543–550.
5. Sarkar, J. (2010). Geometric parameter optimization of ejector – expansion refrigeration cycle with natural refrigerants. *International Journal of Energy Research, 34*, 89–94.
6. Bilir, N., & Ersoy, H. K. (2009). Performance improvement of the vapor compression refrigeration cycle by a two- phase constant area ejector. *International Journal of Energy Research, 33*, 469–480.
7. Disawas, S., & Wongwises, S. (2004). Experimental investigation on the performance of the refrigeration cycle using a two phase ejector as an expansion device. *Int. J. Refrigeration, 27*, 587–594.
8. Hadi, R., Javad, R., Pouria, S. M., & Hadi, G. (2018). Novel dual-loop bi-evaporator vapor compression refrigeration cycles for freezing and air-conditioning applications. *Applied Thermal Engineering, 138*, 563–582.
9. Li, C., Yan, J., Li, Y., Cai, W., Lin, C., & Chen, H. (2016). Experimental study on a multi-evaporator refrigeration system with variable area ratio ejector. *Applied Thermal Engineering, 102*, 196–203.
10. Sarkar, J. (2010). Performance characteristics of multi-evaporator transcritical CO_2 refrigeration cycles with hybrid compression/ejection. *Proceedings of IMechE, Part A, Journal of Power and Energy, 224*(6), 773–780.
11. Lawrence, N., & Elbel, S. (2012). Experimental and analytical investigation of automotive ejector air conditioning cycles using low-pressure refrigerants. *Proceedings of International Air Conditioning and Refrigeration Conference at Purdue* (p. Paper 2118)
12. Lawrence, N., & Elbel, S. (2014). Experimental investigation of a two-phase ejector cycle suitable for use with low-pressure refrigerants R134a and R1234yf. *International Journal of Refrigeration, 38*, 310–322.
13. Latra, B., Philippe, H., & Andre, L. (2014). Investigation of a novel ejector expansion refrigeration system using the working fluid R134a and its potential substitute R1234yf. *International Journal of Refrigeration, 45*, 148–159.
14. Unal, S. (2015). Determination of the ejector dimensions of a bus air-conditioning system using analytical and numerical methods. *Applied Thermal Engineering, 90*, 110–119.
15. Jeon, Y., Kim, D., Jung, J., Jang, D. S., & Kim, Y. (2018). Comparative performance evaluation of conventional and condenser outlet split ejector-based domestic refrigerator-freezers using R600a. *Energy, 161*, 1085–1095.
16. Gao, Y., He, G., Cai, D., & Fan, M. (2020). Performance evaluation of a modified R290 dual-evaporator refrigeration cycle using two-phase ejector as expansion device. *Energy, 212*, 118614.
17. Zilio, C., Brown, J. S., Schiochet, G., & Cavallini, A. (2011). The refrigerant R1234yf in air conditioning systems. *Energy, 36*, 6110–6120.
18. Minor B., Spatz M., (2008) HFO-1234yf low GWP refrigerant update, Proceedings of International Refrigeration and Air Conditioning Conference, Paper 937. http://docs.lib.purdue.edu/iracc/937.
19. Jarall, S. (2012). Study of refrigeration system with HFO-1234yf as a working fluid. *International Journal of Refrigeration, 35*, 1668–1677.
20. Navarro-Esbri, J., Mendoza-Miranda, J. M., Mota-Babiloni, A., & Barraga´n-Cervera A, Belman-Flores AJM. (2013). Experimental analysis of R1234yf as a drop-in replacement for R134a in a vapor compression system. *International Journal of Refrigeration, 36*, 870–880.
21. Elakdhar M., Nehdi E. & Kairouani L., (2007). Analysis of a compression/ Ejection Cycle for domestic refrigeration. *Industrial & Engineering Chemistry Research, 46*, 4639–4644. https://doi.org/10.1021/ie070377e.
22. El-Dessouky, H., Ettouney, H., Alatiqi, I., & Al-Nuwaibit, G. (2002). Evaluation of steam jet ejectors. *Chemical Engineering and Processing, 41*, 551–561.
23. Pridasawas, W. (2006). *Solar-driven refrigeration systems with focus on the ejector cycle (Doctoral Thesis)*. Royal Institute of Technology, KTH.
24. Sun, D. W., & Eames, I. W. (1996). Performance characteristics of HCFC-123 ejector refrigeration cycles. *International Journal of Energy Research, 20*, 871–885.
25. Engineering Equation Solver, Version 10.836-3D, F-Chart Software. https://www.fchart.com/.
26. Yu, J. L., Ren, Y. F., Chen, H., & Li, Y. Z. (2007). Applying mechanical subcooling to ejector refrigeration cycle for improving the coefficient of performance. *Energy Conversion Management, 48*, 1193–1199.
27. Sarkar, J. (2017). Performance analyses of novel two-phase ejector enhanced multi-evaporator refrigeration systems. *Applied Thermal Engineering, 110*, 1635–1642.
28. Chen, J., Havtun, H., & Palm, B. (2014). Investigation of ejectors in refrigeration system. *Applied Thermal Engineering, 64*, 182–191.
29. Li, H., Cao, F., & c., Xianbiao Bu., Lingbao Wang., Xianlong Wang,., (2014). Performance characteristics of R1234yf ejector-expansion refrigeration cycle. *Applied Energy, 121*, 96–103.

Publisher's Note

Springer Nature remains neutral with regard to jurisdictional claims in published maps and institutional affiliations.